Radiol med (2018) 123:143–152
https://doi.org/10.1007/s11547-017-0814-y

ONCOLOGY IMAGING

Analysis of histological findings obtained combining US/mp-MRI fusion-guided biopsies with systematic US biopsies: mp-MRI role in prostate cancer detection and false negative

Eliodoro Faiella[1] · Domiziana Santucci[1] · Federico Greco[1] · Giulia Frauenfelder[1] · Viola Giacobbe[2] · Giovanni Muto[3] · Bruno Beomonte Zobel[1] · Rosario Francesco Grasso[1]

Received: 18 July 2017 / Accepted: 13 September 2017 / Published online: 10 October 2017

Abstract

Aims and objectives To evaluate the diagnostic accuracy of mp-MRI correlating US/mp-MRI fusion-guided biopsy with systematic random US-guided biopsy in prostate cancer diagnosis.

Materials and methods 137 suspected prostatic abnormalities were identified on mp-MRI (1.5T) in 96 patients and classified according to PI-RADS score v2. All target lesions underwent US/mp-MRI fusion biopsy and prostatic sampling was completed by US-guided systematic random 12-core biopsies. Histological analysis and Gleason score were established for all the samples, both target lesions defined by mp-MRI, and random biopsies. PI-RADS score was correlated with the histological results, divided in three groups (benign tissue, atypia and carcinoma) and with Gleason groups, divided in four categories considering the new Grading system of the ISUP 2014, using *t* test. Multivariate analysis was used to correlate PI-RADS and Gleason categories to PSA level and abnormalities axial diameter. When the random core biopsies showed carcinoma (mp-MRI false-negatives), PSA value and lesions Gleason median value were compared with those of carcinomas identified by mp-MRI (true-positives), using *t* test.

Results There was statistically significant difference between PI-RADS score in carcinoma, atypia and benign lesions groups (4.41, 3.61 and 3.24, respectively) and between PI-RADS score in Gleason < 7 group and Gleason > 7 group (4.14 and 4.79, respectively). mp-MRI performance was more accurate for lesions > 15 mm and in patients with PSA > 6 ng/ml. In systematic sampling, 130 (11.25%) mp-MRI false-negative were identified. There was no statistic difference in Gleason median value (7.0 vs 7.06) between this group and the mp-MRI true-positives, but a significant lower PSA median value was demonstrated (7.08 vs 7.53 ng/ml).

Conclusion mp-MRI remains the imaging modality of choice to identify PCa lesions. Integrating US-guided random sampling with US/mp-MRI fusion target lesions sampling, 3.49% of false-negative were identified.

Keywords Prostate cancer lesions · Prostate mp-MRI · PI-RADS score · mp-MRI/US fusion biopsy · US random core biopsy

✉ Eliodoro Faiella
e.faiella@unicampus.it

Domiziana Santucci
d.santucci@unicampus.it

Federico Greco
f.greco@unicampus.it

Giulia Frauenfelder
g.frauenfelder@unicampus.it

Viola Giacobbe
violagiacobbe@yahoo.it

Giovanni Muto
g.muto@unicampus.it

Bruno Beomonte Zobel
b.zobel@unicampus.it

Rosario Francesco Grasso
r.grasso@unicampus.it

[1] Department of Radiology, University of Rome "Campus Bio-medico", Via Alvaro del Portillo, 21-00128 Rome, Italy

[2] Department of Bio-Engineering, University of Rome "Gemelli", Largo Agostino Gemelli, 8, 00168 Rome, Italy

[3] Department of Urology, University of Rome "Campus Bio-medico", Via Alvaro del Portillo, 21-00128 Rome, Italy

Introduction

Prostate cancer (PCa) is the second most common disease and the second cause of cancer-related death in men [1]. Approximately, 14.0% of men will be diagnosed with prostate cancer at some point during their lifetime, based on 2010–2012 data [2].

Definite diagnosis of the existence of PCa is given by histological analysis, which provides the clinician with information on the Gleason score that correlates with PCa prognosis, obtained by biopsies on suspect areas [3]. The first application technique, introduced for the first time in 1989 [4], was a single biopsy of a target nodule identified by ultrasound examination [5]. The current standard technique for a prostate biopsy is random transrectal ultrasound (TRUS)-guided needle insertion, which consists of taking from 10 to 14 cores; this approach leads to a cancer detection rate that ranges from 27 to 40.3% [6, 7].

However, this methodology is not completely accurate and presents several limitations. TRUS biopsy yields upgrading of PCa in at least 25% of patients: identification of microfocal "cancers" of little clinical significance determines a potential problem in men with suspect PCa, which could undergo unnecessary surgical treatment [8, 9]. On the other hand, standard TRUS biopsy undersamples sites far from the needle access (anterior gland), and false negatives are represented by nearly 35% of cases [10] [11].

Magnetic Resonance Imaging (MRI) [12, 13] is recommended by the European Association of Urology (EAU), National Comprehensive Cancer Network (NCCN) and European Society of Urogenital Radiology (ESUR) guidelines in patients with persistently elevated or incremented PSA levels, and/or previous negative biopsies. The aim is to evaluate the gland and identify lesions which could undergo target biopsy [14, 15], in a population including men in active surveillance programs (AS). Many authors have underlined the role of this method and its clinical potential in increasing accuracy of the biopsy, by yielding information and assisting clinicians in the selection of men who might not benefit from biopsies alone [12, 14, 16, 17].

The use of multiparametric MRI (mp-MRI) has shown to reduce the risk of overdetection and overtreatment of non significant lesions and to improve the early detection of clinically significant PCa [18, 19].

Hoeks et al., by working with 3-T multiparametric MRI and a body coil, detected twice as many cancers with targeted biopsy as others have reported using conventional ultrasound guidance (detection rate of 41 vs. 18%). On the other hand, with MRI-targeted biopsies, the detection rate of insignificant cancers, are lower than with systematic blind biopsy [20].

The combination of mp-MRI images with ultrasound real-time techniques allows for the integration of the high sensitivity and negative predictive value given by mp-MRI with the advantages of transrectal ultrasound [20].

Despite the large volume of literature describing the different techniques used to detect and confirm prostate cancer, there continues to be great attention on how to obtain optimal results by selecting the most suitable diagnostic tool. In this sense, the aim of this study was to evaluate the performance of mp-MRI in the detection of prostate lesions and the characterization of the malignant ones, as determined by correlating such data with histological findings obtained through ultrasound fusion biopsy. We also performed prostatic sampling through TRUS-guided random biopsies to analyze false-negative cases and identify in which cases mp-MRI could be inaccurate.

Materials and methods

In this retrospective study, approved by the ethical committee of the Campus Bio-Medico University where patients were tested, we evaluated 96 prostate mp-MRI examinations which were performed at the Department of Radiological Sciences for biochemical or clinical suspects of PCa, between October 2015 and June 2016. Only patients who underwent mp-MRI/TRUS fusion target biopsy were included. All patients were biopsy naïve.

Mp-MRI examinations were performed using a 1.5T scanner (Magnetom Aera Siemens Erlangen, Germany) by positioning a dedicated six-channel body coil over the pelvis, with the patient in the supine position. After localizer sequences were taken in three orthogonal planes, the following protocol was adopted:

1. Sagittal T2-weighted Turbo Spin Echo;
2. Coronal T2-weighted Turbo Spin Echo;
3. Axial T2- weighted Turbo Spin Echo;
4. Axial T1-weighted Turbo Spin Echo;
5. Axial T2-weighted Spectral Attenuated Inversion Recovery;
6. CIS-3D SE PROSTATE; three-dimensional Chemical Shift Imaging Magnetic Resonance Spectroscopy acquires in a number of spectra proportional to the voxel contained in the 2D or 3D matrix;
7. Axial single shot echo-planar diffusion-weighted sequence with diffusion-sensitizing gradient applied along the x, y, z axes and with a b value of 50, 500, 800 and 1000 s/mm^2.
8. Axial T1-weighted dynamic volumetric interpolated breath-hold examination (VIBE) fat suppressed sequence. The contrast agent, gadobenate-dimeglumine (Multihance®; Bracco Imaging, Milan, Italy), was administered in a concentration of 0.2 mmol/kg; it was injected with an automatic injector through a 20

G intravenous cannula at the rate of 4 ml/s, followed by infusion of 15 ml saline solution at the same speed. The contrast agent and the sequence started simultaneously to assess the perfusion of the organ. The sequence was acquired once before and 18 times after the contrast injection (echo trains), for a total duration of 3.7 ± 0.5 min. Subtracted images were automatically derived from DCE-MRI.

9. Axial T1-weighted VIBE Fat Suppressed sequence.

Technical parameters for each sequence are summarized in Table 1.

Each exam had a duration of 31.46 ± 7.2 min.

Following image acquisition, the exams were transferred to a dedicated workstation (Syngo.via, Siemens, Erlangen, Germany); each mp-MRI exam was preliminarily evaluated by two experienced radiologists, and the prostate suspicious lesions were identified.

All lesions were classified using the PI-RADS version 2 lexicon [21], on the basis of morphological and functional findings.

PI-RADS version 2 uses a 5-point scale based on the likelihood that a combination of mp-MRI findings on high resolution T2-weighted (T2W), diffusion-weighted MRI (DWI), and dynamic contrast-enhanced MRI (DCE) correlates with the presence of a clinically significant cancer for each lesion in the prostate gland [18, 22].

All the patients with a suspicious prostate cancer lesion (PI-RADS 4 and 5 and PI-RADS 3, sustained by significant clinical data) underwent MRI-TRUS fusion biopsy. Following assessment by dedicated radiologists, the mp-MRI exams were stored in a CD-ROM, imported on the navigation system (Urostation Koelis, Grenoble, France) and fused with real time ultrasound images.

During TRUS scanning, an acquisition of a transverse section of the prostate was locked and the corresponding axial mp-MRI image was identified, using three anatomical target points as reference: prostate apex, base and posterior edge. The prostate contouring was then performed manually. Once images were locked together, the two methodologies were automatically synchronized. The navigation system allowed to perform an ultrasound exam following the study on mp-MRI imaging in real time. The movement of the US endorectal probe was synchronized with the mp-MRI images which could also be adjusted in the 3D volume to correspond to US images even in oblique plans.

The biopsies were performed on the MRI/US fusion target lesions, previously identified on mp-MRI images, and on other 12 random cores (cranial right, basal right, equator 1 right, equator 2 right, caudal right, apex right, cranial left, basal left, equator 1 left, equator 2 left, caudal left, apex left) an average of four cores were obtained for each target lesion biopsy. The obtained samples were analyzed by a pathologist with at least 10 years of experience.

Based on cell morphology and dysplasia grading, lesions were histopathologically classified in three groups: malignant lesions, atypia or high-grade prostatic intraepithelial neoplasia, and benign prostate tissue [3, 23].

For the histological pattern classification of malignant lesions, we considered the International Society of Urological Pathology (ISUP) 2014 Consensus Conference on Gleason Grading of Prostatic Carcinoma, which split the Gleason score of 7 into two groups, 3 + 4 (called group grade 2) versus 4 + 3 (called group grade 3); we based this criteria on the current data which indicate a worse prognosis for the second group [24]. In our study, we divided lesions into 4 classes, based on the Gleason score: < 7, 7a (obtained by sum of 3 + 4), 7b (obtained by sum of 4 + 3), and > 7.

Table 1 Study protocol adopted for multiparametric MRI (mp-MRI) at 1.5T

Sequence	Slice thickness (mm)	TR (ms)	TE (ms)	Voxel size (mm)	FoV (mm)	Nex	Concatenation
Sagittal T2 TSE	3.0	4000.0	114.0	0.7 × 0.7 × 3	180 × 180	2	2
Coronal T2W TSE	3.0	4400.0	114.0	0.7 × 0.7 × 3	180 × 180	2	2
Axial T2W TSE	3.0	4000.0	114.0	0.7 × 0.7 × 3	180 × 180	2	2
Axial T1W TSE	3.0	568.0	11.0	0.8 × 0.8 × 3	200 × 200	2	2
Axial T2W STIR	3.0	5310.0	95.0	0.8 × 0.8 × 3	200 × 200	2	2
CIS3D SE	4.0	690.0	120.0	0.8 × 0.8 × 0.8		7	
Axial SSEP DWI	4.0	4300.0	73.0	0.9 × 0.9 × 0.9	240 × 240		1
Axial T1W DCE VIBE FSE	4.0	4.46	1.63	1.2 × 1.2 × 4	260 × 260	1	1
Axial T1W VIBE FSE	2.0	4.76	1.82	1 × 1 × 1	200 × 200	2	1

TE time of echo, *TR* time of repetition, *TSE* turbo spin echo, *STIR* short tau inversion recovery, *VIBE* volumetric interpolated breath-hold examination, *FSE* fast spin echo

Lesions were also divided according to PSA serum level (< 10 ng/ml and ≥ 10 ng/ml) and lesions maximum diameter on axial planes (< 15 mm and ≥ 15 mm).

The statistical comparison between PI-RADS score, considered as a non-parametric variable, and the histological results was carried out using the *t* test, to evaluate mp-MRI accuracy in predicting lesion characteristics.

Subsequently, statistical comparisons between PI-RADS scores and Gleason scores were carried out using the *t* test, to evaluate mp-MRI accuracy in predicting histological behaviour in malignant lesions.

Bonferroni test was used to perform a multivariate analysis correlating PI-RADS and Gleason score to PSA levels and lesions maximum diameter on axial planes.

The carcinomas foci identified by random sampling US-guided biopsies, which, therefore, represented mp-MRI false-negatives, were also analyzed. Student *t* test was used to compare PSA values, lesions maximum dimensions and lesions Gleason median value of this group with PSA value, lesions maximum dimension and lesions Gleason median value of PCa identified by mp-MRI (true-positives).

Statistical significance was set at $p < 0.05$. All statistical analysis was performed using the IBM statistical package for social sciences (SPSS, version 18).

Results

The mean age of patients was 66.9 years (SD 7.9; range between 45 and 84 years); the mean PSA level at the time of the biopsy was 14.1 (SD 3.5; range between 0.29 and 29.2 ng/ml).

Considering the prostate tissue histological characteristics, of the 137 target lesions, 71 (51.82%) were carcinoma (group A), 13 (9.49%) were atypia or high grade prostatic intraepithelial neoplasia (group B) and 53 (38.69%) were reported as benign prostate tissue (group C). The mean value of PI-RADS was 4.41 (SD = 0.60) for group A, 3.61 (SD = 0.87) for group B, and 3.24 (SD = 0.81) for group C, as shown in Fig. 1.

The differences between group A and group B, between group B and group C, and between group A and group C were statistically significant.

The median Gleason score of cancer-positive targets was 3 + 4 (range, 3 + 3 to 4 + 5) in group A. Lower grade cancer (Gleason score < 7) (group 1) was identified in 16 of 71 (22.54%) cancer-positive targets (G3 + 3); Gleason score classified as 7a (G3 + 4) (group 2) was identified in 27 of 71 (38.02%) lesions; Gleason score classified as 7b (G4 + 3) (group 3) was identified in 14 of 71 (19,72%) lesions; higher grade cancer (Gleason score > 7) (group 4) was identified in 14 of 71 (19.72%) cancer-positive targets (G4 + 4, 8 targets; G4 + 5, 5 targets; G5 + 4, 1 target).

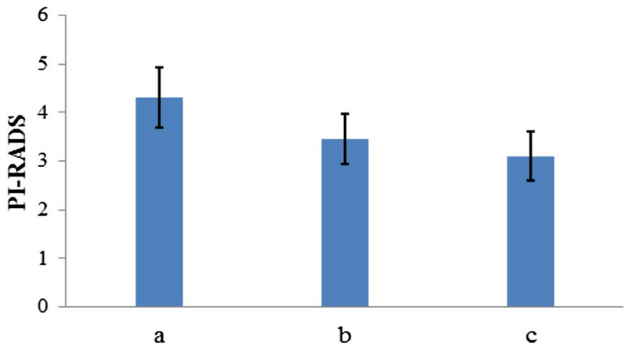

Fig. 1 The chart shows PI-RADS value in the three histological groups. The standard deviation is also reported (**a** malignant lesions; **b** atypia or high-grade prostatic intraepithelial neoplasia; **c** benign prostate tissue)

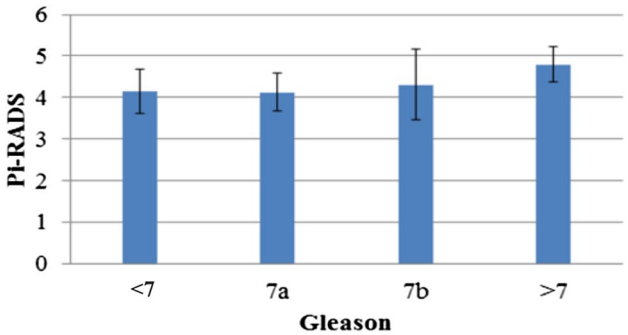

Fig. 2 The chart shows PI-RADS value in the four Gleason groups. The standard deviation is also reported

The mean value of PI-RADS was 4.14 (SD = 0.53) for group 1, 4.12 (SD = 0.45) for group 2, 4.31 (SD = 0.85) for group 3, and 4.79 (SD = 0.42) for group 4, as shown in Fig. 2. The only statistically significant difference was found between group 1 and group 4.

For carcinoma lesions, the median PSA correlated to the Gleason score as follows: 5.65 ng/ml (range 1.1–10.5 ng/ml) in Gleason group 1; 6.15 ng/ml (range 2.4–11.2 ng/ml) in Gleason group 2; 6.72 ng/ml (range 0.29–16.3 ng/ml) in Gleason group 3; and 13.19 ng/ml (range 4.07–35.5 ng/ml) in Gleason group 4.

The only two groups of patients showing a significantly different median value of PI-RADS were the ones with a low PSA level and GS ≤ 7, and with high PSA levels and GS > 7. No statistically significative difference was observed in PI-RADS median value between the group with low PSA and GS > 7 and other groups, neither was it found between groups with high PSA and GS ≤ 7 and other groups. The results of the multivariate analysis are reported in Fig. 3.

For carcinoma lesions, the median lesions maximum diameter value on axial planes correlated to the Gleason

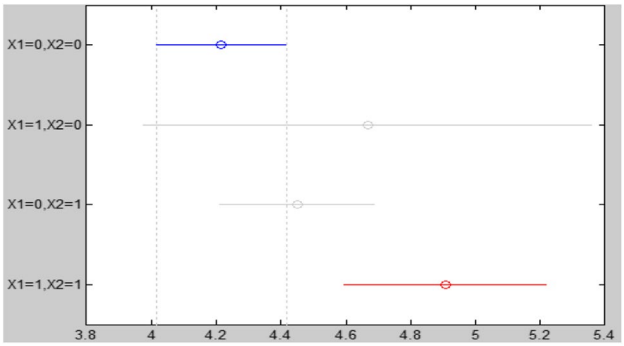

Fig. 3 The chart shows the multivariate analysis, using Bonferroni test. Population was split in four groups considering the Gleason score [*X*1; ≤ 7 (0) and > 7 (1)] and the lesion size [*X*2 < 15 mm (0) and ≥ 15 mm (1)]: group 0,0 (Gleason ≤ 7 and lesion size < 15 mm), group 1,0 (Gleason > 7 and lesion size < 15 mm), group 0,1 (Gleason ≤ 7 and lesion size ≥ 15 mm), group 1,1 (Gleason > 7 and lesion size ≥ 15 mm). The population marginal means of groups 0,0 and 1,1 were significantly different (Bonferroni test)

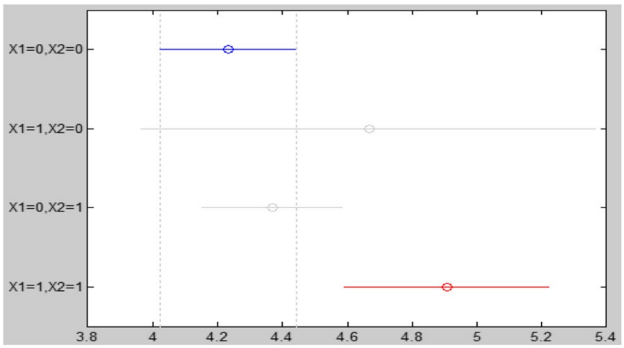

Fig. 4 The chart shows the multivariate analysis, using Bonferroni test. Population was split in four groups considering the Gleason score [*X*1; ≤ 7 (0) and > 7 (1)] and the PSA level [*X*2; < 6 ng/ml (0) and ≥ 6 ng/ml (1)]: group 0,0 (Gleason ≤ 7 and PSA < 6 ng/ml), group 1,0 (Gleason > 7 and PSA < 6 ng/ml), group 0,1 (Gleason ≤ 7 and PSA ≥ 6 ng/ml), group 1,1 (Gleason > 7 and PSA ≥ 6 ng/ml). The population marginal means of groups 0,0 and 1,1 were significantly different (Bonferroni test)

score as follows: 11.94 mm (range 6–20 mm) in Gleason group 1; 13.22 mm (range 5–27 mm) in Gleason group 2; 15.57 mm (range 7–30 mm) in Gleason group 3; and 20 mm (range 9–35 mm) in Gleason group 4.

The only two groups showing a statistically significant different PI-RADS median value were the groups with a smaller diameter and Gleason ≤ 7 and the group with a larger diameter and Gleason > 7. No statistically significant difference was observed in PI-RADS median value between the group with smaller diameter and Gleason > 7 and other groups, or between the group with larger lesions and Gleason ≤ 7 and other groups. The results of the multivariate analysis are reported in Fig. 4.

In a total of 1152 (12 samples × 96 patients) random US-guided systematic biopsies, only 40 cases (3.47%) out of 18 patients showed the presence of carcinoma (mp-MRI false negative).

Also, all the 40 foci showed a Gleason score lower or equal to the Gleason score of the target lesion in the same patient, except for one random biopsy, which showed a lesion with a Gleason score of 8 compared to the target lesion which showed a Gleason of 7 (4 + 3).

Between the mp-MRI false-negative group and the mp-MRI true-positives, there was no significantly statistic difference in the Gleason median value (7.0 vs 7.06), while a significant lower PSA median value (7.08 vs 7.53 ng/ml) and a lower median maximum diameter of the lesions (7.2 vs 21.1 mm) were demonstrated.

Discussion

The importance of the prostate biopsy in the diagnosis of PCa is a well-established concept in literature [22].

The current standard of care in clinical practice for a first time prostatic biopsy involves the acquisition of 10–14 random cores by US-guide sampling, which results in a cancer detection rate of 27–40.3%. In particular, Serefoglu et al. found that the false-negative rate associated to the 12-core prostate biopsy technique was higher than 30% [25]. Therefore, in the past couple of decades, in literature, a tendency to increase the number of cores was expressed, to sample undetected foci of carcinoma and reduce the false-negative rate. Yet the evaluation of detection rates of 18-, 20- and 24-random cores prostatic biopsies, besides the advantage of a more accurate cancer detection rate [26–28], demonstrated an increase of risks and complications (such as bleeding, urinary obstruction, vasovagal reaction and infection). In this context, the fusion of US examination with images of a previous mp-MRI prostatic evaluation, has been proposed [5, 18, 29, 30], to increase the diagnostic accuracy of US random biopsies in the detection of occult prostatic lesions, as well as to identify clinically significant high-risk tumors.

Mp-MRI has gained an important and well-established role in the characterization of PCa lesions by providing a useful tool to predict lesions behaviour, based on the evaluation of different features such as high cell densities (expressed by DWI/ADC sequences), morphological variation of glandular tissue (visualized by T2 signal intensity) and neoangiogenesis (expressed by DCE) [18, 19, 23].

In accordance with the data available in literature, our results showed that the PI-RADS scores obtained through the evaluation of mp-MRI prostate exams, correlates with the macroscopic nature of the examined lesion, and distinguishes benign from malignant tissue.

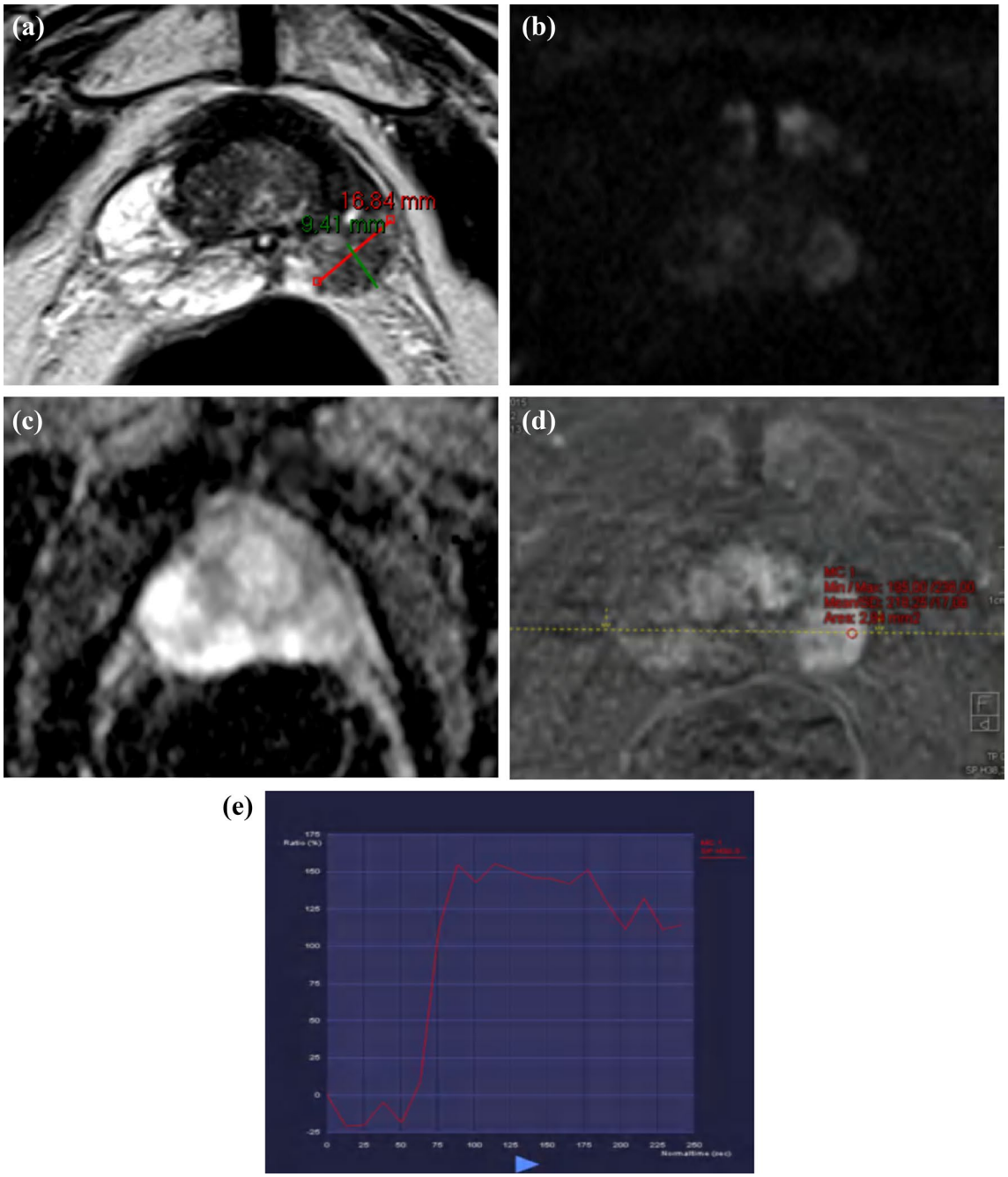

Fig. 5 MRI prostate exam in a 74-year-old patient with PSA of 11,6 ng/ml. T2WI (**a**) shows a hypointense, round-shaped nodule of low SI in the anterior peripheral zone of about 16x9 mm of diameter (arrow). The lesion demonstrates high SI on the high-b-value image of the DWI (**b**) (arrow), low ADC value (**c**) (arrow), strong contrast enhancement (**d**) with early and high peak enhancement with washout on the DCE curve (**e**). The corresponding PI-RADS was 4. The histological result of mp-MRI/US guided biopsy of target lesion confirmed a Gleason 8 (4 + 4) PCa

We also demonstrated that the PI-RADS scores correlate with microscopic features of cancer lesions, based on Gleason classification, with the best capability to distinguish very aggressive lesions (Gleason > 7) from slightly aggressive lesions (Gleason < 7). The performance of mp-MRI, expressed in term of PI-RADS score, decreases in the evaluation of carcinoma with intermediate behaviour, classified as Gleason 7 (group grade 2 and group grade 3). In agreement with the literature [31–33], Gleason 7 carcinoma harbors an element of high-grade pattern carcinoma, and it is intermediate in clinical aggressiveness between patterns group grade 1 and group grade 4 and 5. It has been

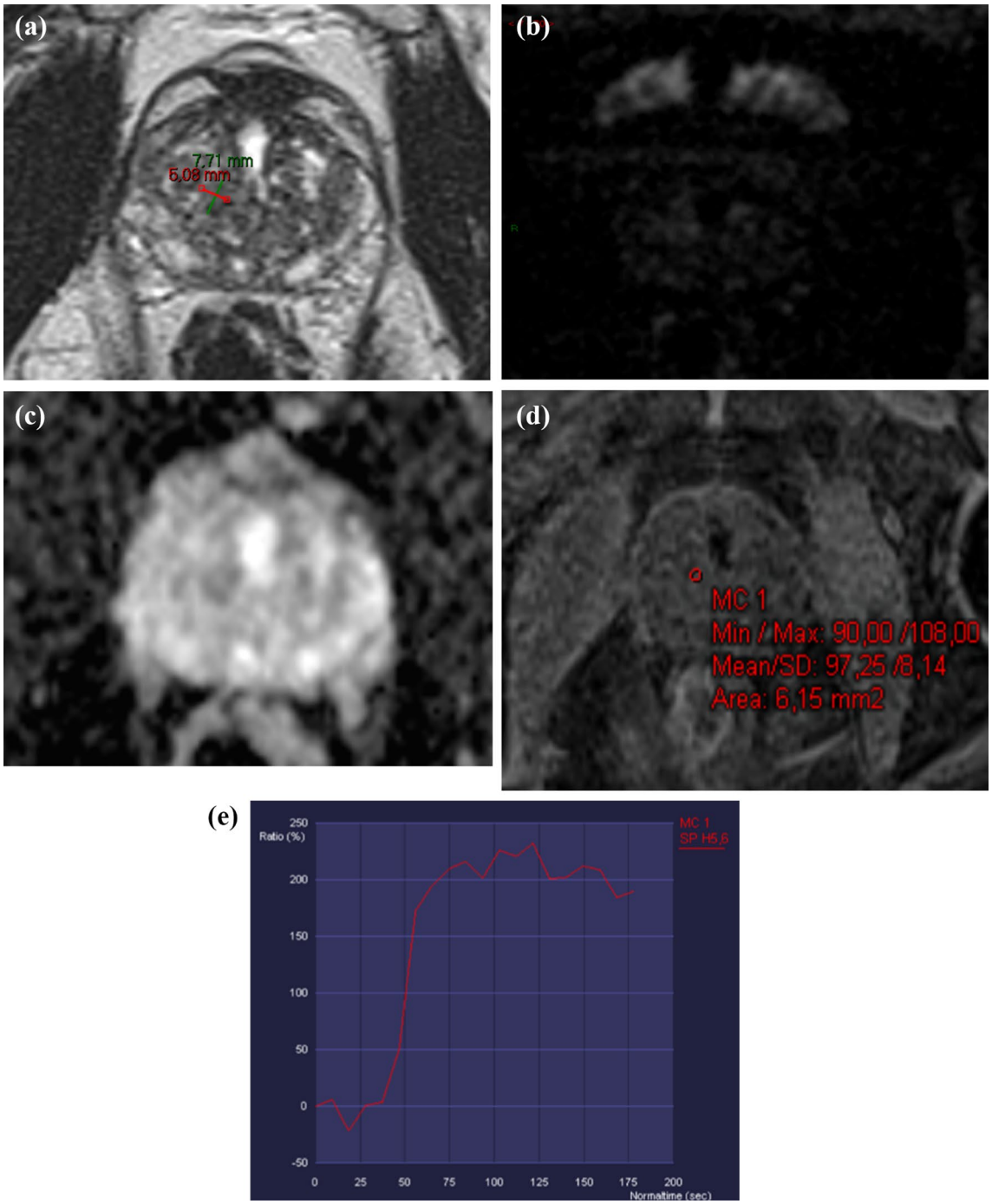

Fig. 6 MRI prostate exam in a 64-year-old man with a PSA of 3.5 ng/ml (increasing from 1.1 in 1 year) and two negative prior biopsies. In the contest of the equator right side adenoma T2 W sequence shows a little and insidious focal hypointense area (**a**) (arrow). The area has reduced ADC but isointense SI on b-1000 DW images (**b**, **c**) (arrow). On DCE there was no suspicious contrast enhancement (**d**) and the DCE curves show a linear pattern (**e**). The corresponding PI-RADS was 3. A clinically significant PCa could not be excluded and the mp-MRI/Us fusion biopsy was executed. The histological result confirmed a Gleason 6 (3 + 3) PCa

demonstrated that all men with Gleason less than 7 and many men with Gleason 7 (3 + 4) could be considered low grade cancer and could be object of active surveillance or radical prostatectomy without requiring pelvic lymph node removal, due to low risk of diffusion. On the other hand, men with a Gleason greater than 8 have been considered high risk patients, with higher recurrence percentage, requiring a more aggressive therapeutic choice, such as radio- or

chemotherapy. Partin et al. demonstrated that men with Gleason 8 disease had similar tumor extent to Gleason 7 (4 + 3) rather than Gleason 9–10 [34, 35]. Therefore, the identification of the highest grade lesions will impact on the chance that these patients have for effective cure. Our results demonstrate that the mp-MRI using PI-RADS total score successfully identifies well-differentiated cancer (Fig. 5), which progresses slowly, and poorly differentiated cancer, which progresses rapidly, but it is less successful in subdividing moderately differentiated cancer, which have an intermediate malignant potential (Fig. 6). We investigated the cause of mp-MRI limits and the cases in which mp-MRI missed PCa lesions identification.

Therefore, once mp-MRI detectability was assessed and true positives were analyze, histological results by mp-MRI/US guided target biopsies and histological results by US random sampling core biopsies were compared and mp-MRI false negative lesions behaviour were analyzed.

Several studies have found that MRI/US-fusion biopsy detect PCa in 34–37% of patients with prior negative TRUS biopsies, with one-third of these patients harboring high-grade cancer as defined by a Gleason score > 7 [36].

Prostate cancer is considered multifocal, small, intermingled with benign stroma, and not uniformly distributed within the gland cancer. This is the reason for which the US random biopsy still maintains an important role in the current clinical practice [37]. However, data coming from the literature in all oncological fields, clearly reflect the need to rely on less invasive techniques, while at the same time maintaining maximum accuracy; this is a fundamental concept to avoid unnecessary treatment and overdiagnosis.

If Ting et al. demonstrated that the combination of random US-guided and target mp-MRI/US fusion-guided biopsies doubled the detection of insignificant PCa, when compared to target mp-MRI/US fusion-guided alone [29], on the other hand, Bjurlin et al. showed that a biopsy strategy combining random US-guided with mp-MRI/US-fusion biopsies can also increase the detection rate of significant PCa, when compared to mp-MRI/US-fusion biopsy alone [37]. In our study, 40/1152 (3.49%) cores of the random sampling US-guided biopsies showed the presence of carcinoma, that was otherwise missed on mp-MRI examination. These lesions had a Gleason median value of 7.0 ± 0.8, which expressed an intermediate behaviour. The data analysis from this group of patients, showed that only one target lesion was identified at mp-MRI exam, and a lower PSA value and lower target lesion maximum diameter were demonstrated, compared to PSA level and target lesion maximum diameter of the rest of the population.

In agreement with a recent review, our results showed that mp-MRI detectability is higher for more clinical aggressive lesions [37], since these have a higher metabolism as well as speed of growth, which are parameters directly related to PSA serum level increase and lesion dimension.

Analyzing histologic behaviour of these microfoci of carcinoma, undetected on mp-MRI exams, we demonstrated that they did not have a Gleason score greater than the Gleason of mp-MRI identified lesions. Therefore, these false-negatives did not impact on patient management and did not modify their clinical prognosis. This data is consistent with recent findings from a large prospective study which showed that MRI/US-fusion biopsy can detect as many Gleason 7 or greater tumors, while simultaneously avoiding the detection of 44% of lower grade disease [29].

This study has some limitations. First of all, it was retrospectively performed in a single institution. Second, the study population was relatively small and the Gleason subgroups were not equal in number, with a greater number of lesions in the patient group with a Gleason score of 7 and this may have influenced the accuracy of PI-RADS statistics. However, patients rate for each group is representative of general population and in accordance with other recent works.

Our findings suggest that US/mp-MRI fusion biopsy represents the elective method to perform prostatic biopsy in a safe and efficacy way and that the PI-RADS score significantly correlates with prostatic lesions aggressiveness. As a matter of fact, among all cancer lesions, tumors with a Gleason greater than 7 were associated with a PI-RADS score of 5 out of 32 lesions (23.19% of cases). PI-RADS score resulted more accurate in lesions with maximum diameter larger than 15 mm and in patients with PSA greater than 6 ng/ml. Moreover, with the exception of one case, in each mp-MRI exam, the prostate cancer lesion with the more aggressive behaviour was correctly identified, and, for this reason, the management of patients was not impacted by the few mp-MRI missed lesions.

In conclusion, the data we present may quite confidently state that mp-MRI remains the imaging modality of choice to identify PCa lesions, and to guide target biopsies—due to its high diagnostic accuracy—in clinical impacting cancer lesions identification.

Compliance with ethical standards

Conflict of interest All authors declare that have no conflicts of interest.

Ethical approval Institutional Review Board approval was not required because this is an observational retrospective study, and only existing information collected from human participants are used and there are not any identifiers linking individuals to the data/samples.

Ethical standards This article does not contain any studies with animals performed by any of the authors.

Informed consent Informed consent was obtained from all individual participants included in the study.

References

1. Jemal A, Siegel R, Ward E, Hao Y, Xu J, Thun MJ (2009) Cancer statistics, 2009. CA Cancer J Clin 59:225–249. doi:10.3322/caac.20006
2. American Cancer Society. Information and resources for cancer: breast, colon, lung, prostate, skin. http://www.cancer.org/
3. Buhmeida A, Pyrhönen S, Laato M, Collan Y (2006) Prognostic factors in prostate cancer. Diagn Pathol 1:4. doi:10.1186/1746-1596-1-4
4. Hodge KK, McNeal JE, Stamey TA(1989) Ultrasound guided transrectal core biopsies of the palpably abnormal prostate. J Urol 142:66–70. http://www.ncbi.nlm.nih.gov/pubmed/2659826. Accessed 19 Sept 2016
5. Marks L, Young S, Natarajan S (2013) MRI-ultrasound fusion for guidance of targeted prostate biopsy. Curr Opin Urol 23:43–50. doi:10.1097/MOU.0b013e32835ad3ee
6. Patel AR, Jones JS (2009) Optimal biopsy strategies for the diagnosis and staging of prostate cancer. Curr Opin Urol 19:232–7. http://www.ncbi.nlm.nih.gov/pubmed/19365892. Accessed 19 Sept 2016
7. Xu S, Kruecker J, Turkbey B, Glossop N, Singh AK, Choyke P, Pinto P, Wood BJ (2008) Real-time MRI-TRUS fusion for guidance of targeted prostate biopsies. Comput Aided Surg 13:255–264. doi:10.3109/10929080802364645
8. Carlson GD, Calvanese CB, Kahane H, Epstein JI (1998) Accuracy of biopsy Gleason scores from a large uropathology laboratory: use of a diagnostic protocol to minimize observer variability. Urology 51:525–9. http://www.ncbi.nlm.nih.gov/pubmed/9586600. Accessed 19 Sept 2016
9. Tilki D, Schlenker B, John M, Buchner A, Stanislaus P, Gratzke C, Karl A, Tan GY, Ergün S, Tewari AK, Stief CG, Seitz M, Reich O (2011) Clinical and pathologic predictors of Gleason sum upgrading in patients after radical prostatectomy: results from a single institution series. Urol Oncol 29:508–514. doi:10.1016/j.urolonc.2009.07.003
10. Taira AV, Merrick GS, Galbreath RW, Andreini H, Taubenslag W, Curtis R, Butler WM, Adamovich E, Wallner KE (2010) Performance of transperineal template-guided mapping biopsy in detecting prostate cancer in the initial and repeat biopsy setting. Prostate Cancer Prostatic Dis 13:71–77. doi:10.1038/pcan.2009.42
11. Faiella E, Santucci D, Greco F, Pacella G, Beomonte Zobel B, Grasso FR (2017) Ruolo delle sequenza di Risonanza Magnetica Multiparametrica nelle caratterizzazione delle lesioni prostatiche della zona periferica sospette per carcinoma e valore di PI-RADS 3, Giornale Italiano di Radiologia Medica **(in press)**
12. Turkbey B, Merino MJ, Gallardo EC, Shah V, Aras O, Bernardo M, Mena E, Daar D, Rastinehad AR, Linehan WM, Wood BJ, Pinto PA, Choyke PL (2014) Comparison of endorectal coil and nonendorectal coil T2W and diffusion-weighted MRI at 3 Tesla for localizing prostate cancer: correlation with whole-mount histopathology. J Magn Reson Imaging 39:1443–1448. doi:10.1002/jmri.24317
13. Turkbey B, Albert PS, Kurdziel K, Choyke PL (2009) Imaging localized prostate cancer: current approaches and new developments. AJR Am J Roentgenol 192:1471–1480. doi:10.2214/AJR.09.2527
14. Thompson J, Lawrentschuk N, Frydenberg M, Thompson L, Stricker P, USANZ (2013) The role of magnetic resonance imaging in the diagnosis and management of prostate cancer. BJU Int. doi:10.1111/bju.12381
15. Sciarra A, Barentsz J, Bjartell A, Eastham J, Hricak H, Panebianco V, Witjes JA (2011) Advances in magnetic resonance imaging: how they are changing the management of prostate cancer. Eur Urol 59:962–977. doi:10.1016/j.eururo.2011.02.034
16. Fuchsjäger M, Shukla-Dave A, Akin O, Barentsz J, Hricak H (2008) Prostate cancer imaging. Acta Radiol 49:107–120. doi:10.1080/02841850701545821
17. Kim CK, Park BK (2008) Update of prostate magnetic resonance imaging at 3 T. J Comput Assist Tomogr 32:163–172. doi:10.1097/RCT.0b013e3180683b99
18. Pinto PA, Chung PH, Rastinehad AR, Baccala AA, Kruecker J, Benjamin CJ, Xu S, Yan P, Kadoury S, Chua C, Locklin JK, Turkbey B, Shih JH, Gates SP, Buckner C, Bratslavsky G, Linehan WM, Glossop ND, Choyke PL, Wood BJ (2011) Magnetic resonance imaging/ultrasound fusion guided prostate biopsy improves cancer detection following transrectal ultrasound biopsy and correlates with multiparametric magnetic resonance imaging. J Urol 186:1281–1285. doi:10.1016/j.juro.2011.05.078
19. De Visschere PJL, Briganti A, Fütterer JJ, Ghadjar P, Isbarn H, Massard C, Ost P, Sooriakumaran P, Surcel CI, Valerio M, van den Bergh RCN, Ploussard G, Giannarini G, Villeirs GM (2016) Role of multiparametric magnetic resonance imaging in early detection of prostate cancer. Insights Imaging 7:205–214. doi:10.1007/s13244-016-0466-9
20. Hoeks CMA, Barentsz JO, Hambrock T, Yakar D, Somford DM, Heijmink SWTPJ, Scheenen TWJ, Vos PC, Huisman H, van Oort IM, Witjes JA, Heerschap A, Fütterer JJ (2011) Prostate cancer: multiparametric mr imaging for detection, localization, and staging. Radiology 261:46–66. doi:10.1148/radiol.11091822
21. Röthke M, Blondin D, Schlemmer H-P, Franiel T (2013) PI-RADS classification: structured reporting for MRI of the prostate. Rofo 185(3):253–261. doi:10.1055/s-0032-1330270
22. Hricak H, Choyke PL, Eberhardt SC, Leibel SA, Scardino PT (2007) Imaging prostate cancer: a multidisciplinary perspective. Radiology 243:28–53. doi:10.1148/radiol.2431030580
23. Dianat SS, Carter HB, Schaeffer EM, Hamper UM, Epstein JI, Macura KJ (2015) Association of quantitative magnetic resonance imaging parameters with histological findings from MRI/ultrasound fusion prostate biopsy. Can J Urol 22(5):7965–7972 **PMID: 26432966**
24. Epstein JI, Egevad L, Amin MB, Delahunt B, Srigley JR, Humphrey PA, Grading Committee (2016) The 2014 International Society of Urological Pathology (ISUP) consensus conference on Gleason grading of prostatic carcinoma: definition of grading patterns and proposal for a new grading system. Am J Surg Pathol 40:244–252. doi:10.1097/PAS.0000000000000530
25. Serefoglu EC, Altinova S, Ugras NS, Akincioglu E, Asil E, Balbay MD (2013) How reliable is 12-core prostate biopsy procedure in the detection of prostate cancer? Can Urol Assoc J 7:E293–E298. doi:10.5489/cuaj.11224
26. Pepe P, Aragona F (2007) Saturation prostate needle biopsy and prostate cancer detection at initial and repeat evaluation. Urology 70:1131–1135. doi:10.1016/j.urology.2007.07.068
27. Scattoni V, Roscigno M, Raber M, Dehò F, Maga T, Zanoni M, Riva M, Sangalli M, Nava L, Mazzoccoli B, Freschi M, Guazzoni G, Rigatti P, Montorsi F (2008) Initial extended transrectal prostate biopsy—are more prostate cancers detected with 18 cores than with 12 cores? J Urol 179:1327–1331. doi:10.1016/j.juro.2007.11.052 **(discussion 1331)**
28. Ravery V, Dominique S, Panhard X, Toublanc M, Boccon-Gibod L, Boccon-Gibod L (2008) The 20-core prostate biopsy protocol—a new gold standard? J Urol 179:504–507. doi:10.1016/j.juro.2007.09.033

29. Ting F, Van Leeuwen PJ, Thompson J, Shnier R, Moses D, Delprado W, Stricker PD (2016) Assessment of the performance of magnetic resonance imaging/ultrasound fusion guided prostate biopsy against a combined targeted plus systematic biopsy approach using 24-core transperineal template saturation mapping prostate biopsy. Prostate Cancer 2016:3794738. doi:10.1155/2016/3794738
30. Kongnyuy M, George AK, Rastinehad AR, Pinto PA (2016) Magnetic resonance imaging-ultrasound fusion-guided prostate biopsy: review of technology, techniques, and outcomes. Curr Urol Rep 17:32. doi:10.1007/s11934-016-0589-z
31. Barry MJ, Albertsen PC, Bagshaw MA, Blute ML, Cox R, Middleton RG, Gleason DF, Zincke H, Bergstralh EJ, Jacobsen SJ (2001) Outcomes for men with clinically nonmetastatic prostate carcinoma managed with radical prostatectomy, external beam radiotherapy, or expectant management. Cancer 91:2302–2314. doi:10.1002/1097-0142(20010615)91:12<2302:AID-CNCR1262>3.0.CO;2-P
32. Albertsen PC, Hanley JA, Gleason DF, Barry MJ, G S, DF G, SH L, JE J, GW C, PC A, PC W, ME C, MA B, GS G, JI E, JC B, ME C, JD K, YMM B, M S, G A, J H, PH G, GP M, WJ C, ED C (1998) Competing risk analysis of men aged 55 to 74 years at diagnosis managed conservatively for clinically localized prostate cancer. JAMA 280:975. doi:10.1001/jama.280.11.975
33. J.I. Epstein, A.W. Partin, J. Sauvageot, P.C (1996) Walsh, Prediction of progression following radical prostatectomy. A multivariate analysis of 721 men with long-term follow-up., Am. J. Surg. Pathol. 20:286–92. http://www.ncbi.nlm.nih.gov/pubmed/8772781 (accessed September 27, 2016)
34. A.W. Partin, M.W. Kattan, E.N. Subong, P.C. Walsh, K.J. Wojno, J.E. Oesterling, P.T. Scardino, J.D. Pearson, Combination of prostate-specific antigen, clinical stage, and Gleason score to predict pathological stage of localized prostate cancer. A multi-institutional update., JAMA. 277 (1997) 1445–51. http://www.ncbi.nlm.nih.gov/pubmed/9145716 (accessed September 25, 2016)
35. Weinreb JC, Barentsz JO, Choyke PL, Cornud F, Haider MA, Macura KJ, Margolis D, Schnall MD, Shtern F, Tempany CM, Thoeny HC, Verma S (2015) PI-RADS prostate imaging—reporting and data system: 2015, version 2. Eur Urol 69(2016):16–40. doi:10.1016/j.eururo.2015.08.052
36. Vourganti S, Rastinehad A, Yerram NK, Nix J, Volkin D, Hoang A, Turkbey B, Gupta GN, Kruecker J, Linehan WM, Choyke PL, Wood BJ, Pinto PA (2012) Multiparametric magnetic resonance imaging and ultrasound fusion biopsy detect prostate cancer in patients with prior negative transrectal ultrasound biopsies. J Urol 188:2152–2157. doi:10.1016/j.juro.2012.08.025
37. Bjurlin MA, Mendhiratta N, Wysock JS, Taneja SS (2016) Multiparametric MRI and targeted prostate biopsy: improvements in cancer detection, localization, and risk assessment. Cent Eur J Urol 69:9–18. doi:10.5173/ceju.2016.734